

## The growth mechanisms of graphene directly on sapphire substrates by using the chemical vapor deposition

Meng-Yu Lin, Chen-Fung Su, Si-Chen Lee, and Shih-Yen Lin

Citation: [Journal of Applied Physics](#) **115**, 223510 (2014); doi: 10.1063/1.4883359

View online: <http://dx.doi.org/10.1063/1.4883359>

View Table of Contents: <http://scitation.aip.org/content/aip/journal/jap/115/22?ver=pdfcov>

Published by the [AIP Publishing](#)

---

### Articles you may be interested in

[Temperature dependence of the Raman spectra of polycrystalline graphene grown by chemical vapor deposition](#)  
Appl. Phys. Lett. **105**, 023108 (2014); 10.1063/1.4890388

[Strain relaxation in graphene grown by chemical vapor deposition](#)  
J. Appl. Phys. **114**, 214312 (2013); 10.1063/1.4834538

[Study of the growth of graphene film on Ni and Si substrates by hot filament chemical vapor deposition](#)  
AIP Conf. Proc. **1536**, 545 (2013); 10.1063/1.4810342

[Epitaxial \(111\) films of Cu, Ni, and  \$Cu\_xNi\_y\$  on  \$\alpha-Al\_2O\_3\$  \(0001\) for graphene growth by chemical vapor deposition](#)  
J. Appl. Phys. **112**, 064317 (2012); 10.1063/1.4754013

[Controllable chemical vapor deposition of large area uniform nanocrystalline graphene directly on silicon dioxide](#)  
J. Appl. Phys. **111**, 044103 (2012); 10.1063/1.3686135

---



# The growth mechanisms of graphene directly on sapphire substrates by using the chemical vapor deposition

Meng-Yu Lin,<sup>1,2</sup> Chen-Fung Su,<sup>2</sup> Si-Chen Lee,<sup>1</sup> and Shih-Yen Lin<sup>1,2,3,a)</sup>

<sup>1</sup>Graduate Institute of Electronics Engineering, National Taiwan University, Taipei 10617, Taiwan

<sup>2</sup>Research Center for Applied Sciences, Academia Sinica, Taipei 11529, Taiwan

<sup>3</sup>Department of Photonics, National Chiao Tung University, Hsinchu 30010, Taiwan

(Received 26 February 2014; accepted 3 June 2014; published online 11 June 2014)

Uniform and large-area graphene films grown directly on sapphire substrates by using a low-pressure chemical vapor deposition system are demonstrated in this paper. The evolution process and the similar Raman spectra of the samples with different growth durations have confirmed that the continuous graphene film is formed by graphene flakes with similar sizes. The layer-by-layer growth mechanism of this approach is attributed to the preferential graphene deposition on sapphire surfaces. The etching effect of H<sub>2</sub> gas is demonstrated to be advantageous for the larger graphene grain formation. The smooth surface of substrates is also proved to be a key parameter for continuous graphene film formation with better crystalline quality. © 2014 AIP Publishing LLC. [<http://dx.doi.org/10.1063/1.4883359>]

## I. INTRODUCTION

Since the two-dimensional material graphene was fabricated by using the mechanical exfoliation method at 2004, massive efforts have been devoted to this research area.<sup>1</sup> Among them, most of the effort is focused on the expansion of the graphene film area via different growth methods since only flakes of graphene are obtained by using the mechanical exfoliation approach. At this stage, there are two major approaches, which have been proven to be promising for large-area graphene growth. They are Si sublimation from SiC substrates at high temperatures leaving C atoms on the surface for graphitization and chemical vapor deposition (CVD) for graphene growth on metal templates.<sup>2–4</sup> Although the SiC sublimation method does provide large-area graphene films, the high price of SiC substrates and the only substrate choice would limit the practical application of this approach. Compared with the SiC sublimation method, CVD growth of graphene on metal templates has provided a cheaper and layer number controllable approach to obtain large-area graphene films. Two metals, including Cu and Ni, are commonly chosen in the CVD growth method. Because the graphene film is grown on the metal template, film transfer procedure is required. During the transfer process, damages to the graphene films, including broken holes and doping effect, are usually observed.<sup>5</sup> These damages would reduce the mobility of the graphene transistors and they are difficult to recover. Therefore, an alternate approach to provide transfer-free graphene films on the dielectric substrates is required for the practical applications of the material.

In previous publications, graphene growth underneath pre-deposited Ni or Cu templates on the SiO<sub>2</sub>/Si substrates has been demonstrated.<sup>6–8</sup> These approaches do provide graphene films on dielectric substrates without the common transferring procedure required for CVD grown graphene.

However, the high growth temperature of these approaches may result in the metal template de-wetting and evaporating problem during graphene growth, which would affect the graphene film quality and completeness.<sup>9</sup> The required metal removal procedure via chemical etching of these approaches may also bring in extrinsic doping to the graphene films. It has been demonstrated in previous publications that graphene films can be grown directly on sapphire substrate without using metal catalyst.<sup>10</sup> Due to the graphene films prepared by using this method is composed of nano-scale graphene flakes, high defect density is observed on the film. Although high temperature is still required, both film transferring procedure for CVD-grown graphene or metal removal for underneath graphene can be avoided by using this approach. Another important parameter for graphene growth is the H<sub>2</sub> flow rate during growth. It has been reported elsewhere that the D peak intensity of the directly grown graphene would be greatly affected by the H<sub>2</sub> flow ratios during growth.<sup>11</sup> Therefore, graphene growth directly on sapphire substrates with proper H<sub>2</sub> flow ratios can be an alternate approach for large-area graphene growth without metal catalyst.

In this paper, we have demonstrated the growth of uniform and large-area graphene films directly on sapphire substrates by using the low-pressure CVD (LPCVD) system. The influence of different growth parameters and growth evolution of the films are investigated. The evolution process and the similar Raman spectra of the samples with growth different durations have confirmed that the continuous graphene film is formed by graphene flakes with similar sizes. By changing the H<sub>2</sub> flow ratios during, the etching effect of H<sub>2</sub> gas is demonstrated to be advantageous for the larger graphene grain formation.

## II. EXPERIMENTS

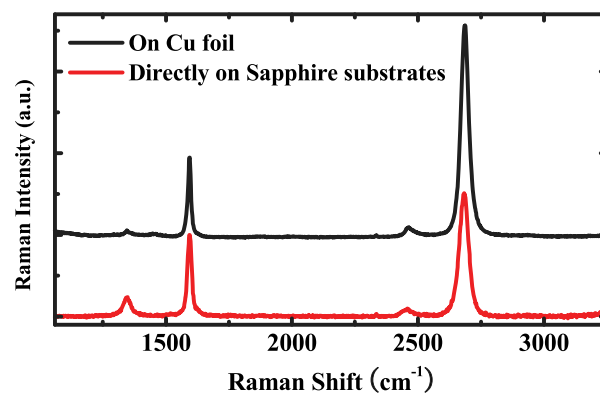
Before growth, sapphire substrates are cleaned with acetone, isopropanol, and de-ionized (DI) water. The substrate

<sup>a)</sup>Author to whom correspondence should be addressed. Electronic mail: shihyen@gate.sinica.edu.tw

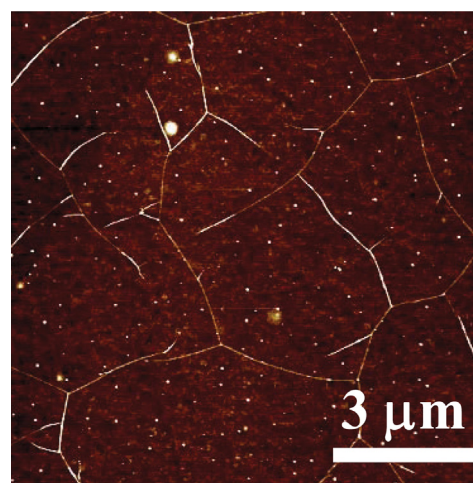
is then annealed in a 1-in. quartz tube furnace system at 1100 °C under Ar environment for 30 min. Since low pressure is required for the sapphire substrate during the high-temperature annealing procedure, the LPCVD technique is adopted for graphene growth.<sup>3</sup> By using the BRUKER Dimension Icon atomic force microscope system (AFM), the surface roughness of the sapphire substrate improves from 0.09 to 0.05 nm after the high-temperature annealing procedure. After the annealing procedure, the Ar, H<sub>2</sub>, and CH<sub>4</sub> mixture gas is introduced into the CVD system to grow graphene films directly on the substrate surface. The flow rates of Ar, H<sub>2</sub>, and CH<sub>4</sub> are set as 200, 200, and 30 sccm, respectively. After 3 h of growth, the sample is removed out of the chamber. The Raman spectra of the graphene films are measured by a HORIBA Jobin Yvon HR800UV Raman spectroscopy system equipped with 532 nm laser. The surface morphologies of the graphene films are studied by using AFM and scanning electron microscope (SEM) systems.

### III. RESULTS AND DISCUSSIONS

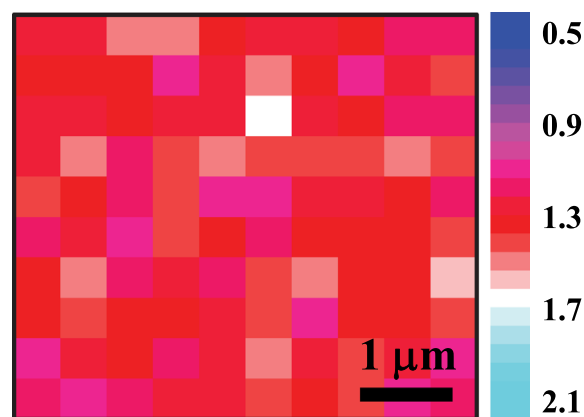
The Raman spectrum of the graphene film grown directly on a sapphire substrate for 3 h is shown in Fig. 1(a). For comparison, the Raman spectrum of the graphene film prepared by using the same method on 25 μm Cu foil and then re-attached to a 300 nm SiO<sub>2</sub>/Si substrate is also shown in the figure. Compared with the film grown on Cu foil, more intense D peak and lower 2D peak located near 1346 and 2684 cm<sup>-1</sup>, respectively, are observed for the film grown directly on the sapphire substrate. The more intense 2D peak of the directly grown graphene film compared with its G peak might suggest that a single-layer graphene can be obtained. However, the similar 2D peak full width at half maximum (FWHM) 43 cm<sup>-1</sup> with the value 45 cm<sup>-1</sup> for the bi-layer graphene film grown on Cu foil suggests that bi-layer graphene should be obtained by using this method.<sup>12</sup> And from the I<sub>D</sub>/I<sub>G</sub> ratio, the graphene flake sizes of the film would be around 83 nm.<sup>13</sup> To investigate the surface morphology of the graphene film grown directly on the sapphire substrate, a 10 × 10 μm<sup>2</sup> AFM image of the film is shown in Fig. 1(b). As shown in the figure, uniform distributed graphene film can be observed on the sample surface. However, due to the different thermal expansion coefficients between graphene and the sapphire substrates, the cooling procedure from the high temperature 1100 °C would result in wrinkle formation on the sample surface. To verify if bi-layer graphene is obtained via this approach, a scratch is fabricated on the film and measured by using AFM. The measured 1.2 nm depth across the scratch edge has confirmed that bi-layer graphene is obtained via this approach.<sup>14</sup> To further investigate the uniformity of the graphene film, Raman mapping over the 5 × 5 μm<sup>2</sup> sample area is performed. The spatial resolution of the mapping is determined by the laser spot size 500 nm. The I<sub>2D</sub>/I<sub>G</sub> ratios over the area are shown in Fig. 1(c). As shown in the figure, quite uniform 2D/G peak ratios are observed, which also suggest a uniform graphene film is obtained via this approach. The results are consistent with the observation of the AFM image shown in Fig. 1(b).



(a)



(b)



(c)

FIG. 1. (a) The Raman spectra of the graphene films prepared by the CVD system on Cu foil and directly on the sapphire substrate, (b) the AFM image of the graphene film grown directly on the sapphire substrate, and (c) the I<sub>2D</sub>/I<sub>G</sub> ratios obtained from the Raman mapping results over the 5 × 5 μm<sup>2</sup> sample area.

To investigate the growth mechanisms of the directly grown graphene, the SEM images of the graphene films grown for 60, 120, 180 and 240 min are shown in Figs. 2(a)–2(d), respectively. The normalized Raman spectra to the G peak of the four samples are shown in Fig. 2(e). As shown in Fig. 2(a), the sapphire substrate (the dark region) can still be observed between the graphene clusters. The

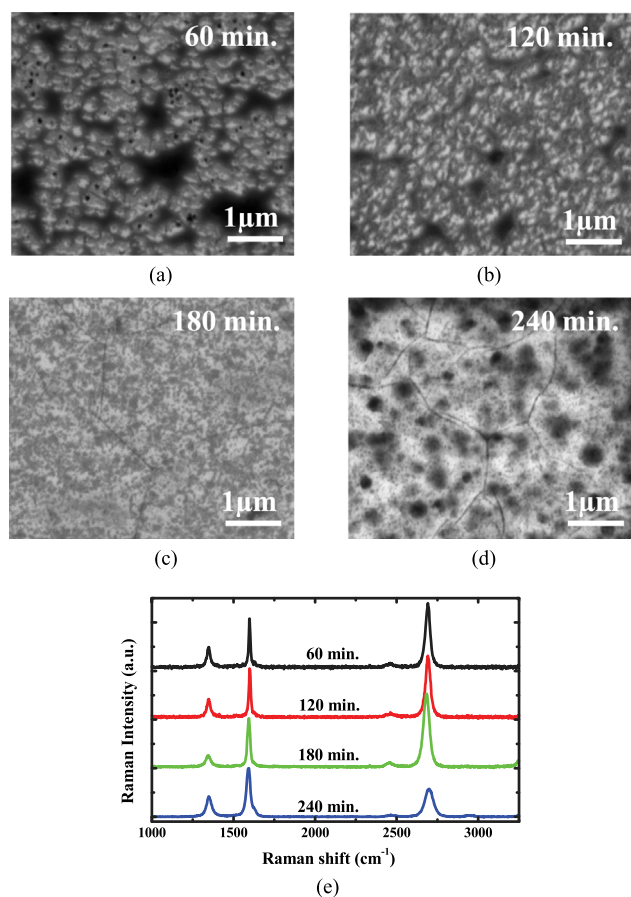


FIG. 2. (a)–(d) The SEM images and (e) Raman spectra of the graphene films grown directly on sapphire substrates with different growth periods. They are 60, 120, 180, and 240 min for figures (a), (b), (c), and (d), respectively.

results suggest that after 1 h of growth, the graphene grains do not fully cover the whole substrate. Compared with the  $\sim 1$  h growth time of fully covered graphene film on Cu foil, the growth rate of direct graphene growth on sapphire substrates is much slower. And since the film shown in Fig. 2(a) is composed of discrete flakes, more intense D peak of the sample is observed in Fig. 2(e) indicating higher defects around the flakes. With increasing growth duration to 120 min, the density of the graphene flakes increases as shown in Fig. 2(b). Although some of the graphene flakes seem to merge with each other, the graphene flake sizes are similar to the sample with 60 min growth duration. The similar D peak intensity ratios of the two samples confirm this point. This result indicates that unlike the growth mechanism of graphene on Cu foil, in which, the graphene growth starts from seeding and then expands to a continuous film,<sup>15</sup> direct graphene growth on sapphire substrates does not seem to undergo lateral growth on substrates. It seems that the graphene grains just fall on the substrates. The limited lateral growth procedure may only take place when the flakes overlap. With further increasing the growth duration to 180 min, the SEM image shown in Fig. 2(c) reveals a continuous graphene film on the entire sapphire substrate. The sheet resistance of the graphene film is  $5.7 \times 10^2 \Omega/\text{sq}$ , which is compatible to the film grown on Cu foil. The slightly lower D peak intensity ratio of the sample suggests that although the film is composed of small graphene grains, the limited

lateral growth at the grain overlapping would still slightly increase the graphene grain sizes. For the sample with even longer growth time 240 min, besides the underlying graphene film, cluster structures are again observed in Fig. 2(d). With the observed higher D peak and lower 2D peak intensity ratios of the sample shown in Fig. 2(e), the results suggest that thicker layer of graphene starts to grow on the graphene film, which is quite different with the self-limited growth process of graphene films on the Cu foil.<sup>3</sup>

One commonly adopted approach to derive the mobility value of the graphene film is to fabricate back-gated graphene transistors. However, since the conventional graphene transferring method cannot be applied to the film grown directly on sapphire substrates, a different transferring procedure<sup>10</sup> is employed as follows: (a) deposit 300 nm Cu on directly grown graphene on sapphire substrates, (b) deposit 500 nm polymethylmethacrylate (PMMA) by using spin coating on the Cu film, (c) peel off the PMMA/Cu/graphene film from sapphire substrates in DI water, (d) reattach the film to a 300 nm  $\text{SiO}_2/\text{Si}$  substrate, and (e) remove the top PMMA and Cu films by using acetone and  $\text{FeNO}_3$  solutions, respectively. After the film transferring, a standard back-gated graphene transistor is fabricated by using photo-lithography. The  $I_D - V_{GS}$  curve of the device is shown in Fig. 3. The inset figure shows the SEM image of the device. The graphene film is prepared under the same conditions of the film shown in the SEM image of Fig. 2(c). As shown in the figure, although the standard graphene transistor behavior is observed, the derived mobility  $35.6 \text{ cm}^2 \text{ V}^{-1} \text{ s}^{-1}$  from the curve is low compared with other devices fabricated by using CVD-prepared graphene. Since low D-peak intensity is observed from the film, the low mobility of the device may be attributed to the increasing defect number on the graphene film induced during the brutal peeling process. To improve the device performances, other transferring procedure for the graphene film grown on sapphire substrates is to be developed in the future.

To further explain the growth mechanisms of the graphene films on sapphire substrates, schematic diagrams of the growth model are shown in Fig. 4. At the initial stage shown in the figure, methane decomposition into C atoms would take place in the atmosphere of the  $1100^\circ\text{C}$  quartz

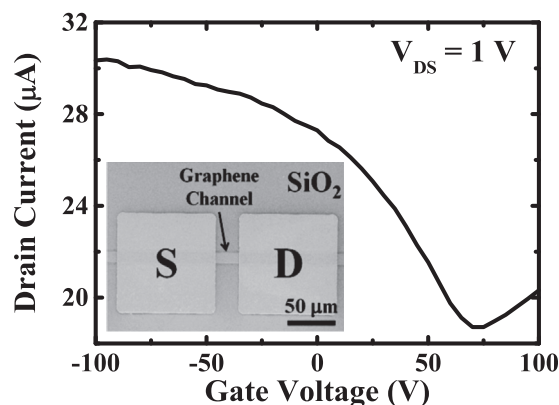


FIG. 3. The  $I_D - V_{GS}$  curve of the back-gated graphene transistor fabricated by using the directly grown graphene on sapphire substrate. The inset figure shows the SEM image of the device.

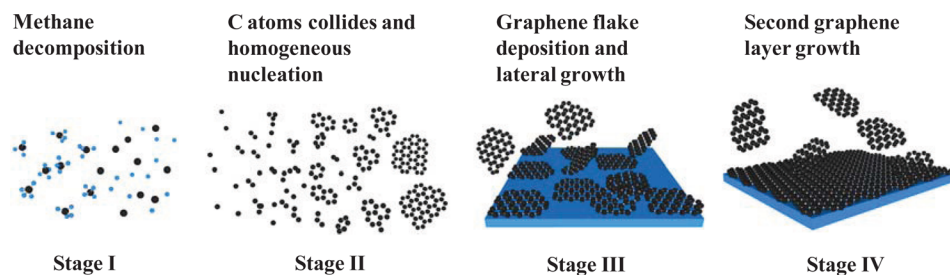


FIG. 4. The schematic diagrams showing the mechanisms of the direct graphene growth on sapphire substrates.

tube.<sup>16</sup> After methane decomposition, the C atoms would collide and undergo homogeneous nucleation. In this case, graphene flakes would be formed in the gaseous environment. The graphene flakes would continue to grow in sizes until they fall on the substrate surfaces. Although there seems to be no preference sites for the graphene flake deposition, the growth evolution shown in Figs. 2(a)–2(d) suggests that the graphene/substrate interface adhesion should be superior to graphene/graphene interfaces. In this case, before the substrate surface is fully covered with graphene, most of the flakes fall on the other graphene flakes would be blown away by the injected gas flow. The limited lateral graphene growth in the flake overlappings would also enhance the crystalline quality of the film at this stage. After the substrate surface is fully covered with graphene, the phenomenon of preferential graphene flake deposition on sapphire surfaces disappears and upper graphene flakes start to deposit on the complete graphene film covering the sapphire substrates. However, due to the lack of preferential graphene deposition, uniform upper layer graphene with high crystalline quality is not available by using this approach as shown in the SEM image of Fig. 2(d) and the higher D peak of Fig. 2(e).

The other parameter affecting graphene growth would be the composition of the flowing gas and the role of H<sub>2</sub> gas during growth. With the flow rate of methane kept at 30 sccm and the total flow rate of H<sub>2</sub> and Ar kept at 400 sccm, four samples grown under different H<sub>2</sub>/Ar flow ratios 50/350, 100/300, 150/250, and 200/200 are prepared. The growth duration of the four samples is set at 60 min. The SEM image of the sample with the H<sub>2</sub>/Ar flow ratio 50/350 is shown in Fig. 5(a). Compared with the SEM image of the sample grown with the H<sub>2</sub>/Ar flow ratio 200/200 and the same growth duration shown in Fig. 2(a), a continuous graphene film fully covers the sapphire substrate instead of separate graphene flakes. The results suggest that with higher H<sub>2</sub> composition in the gas flow during growth, the growth rate of the graphene film would be greatly depressed. The possible mechanism responsible for this phenomenon would be the H<sub>2</sub> etching effect over defective graphene at high growth temperature.<sup>17</sup> In this case, although methane gas flow is the same for the two samples, the H<sub>2</sub> etching effect would effectively decrease the growth rate of the direct graphene growth on sapphire substrates. The same effect may also benefit the formation of larger graphene flakes since smaller ones would be etched off by H<sub>2</sub> gas during growth. The decreasing D peak intensities of the normalized Raman spectra over the G peak intensities shown in Fig. 5(b) of the samples grown with increasing H<sub>2</sub>/Ar ratios have also

confirmed this attribution since the graphene grain size is inverse proportional to the D/G peak ratios.<sup>13,18</sup>

The last major parameter, which might affect the graphene growth would be the substrate choice. With the growth conditions of methane, H<sub>2</sub>, and Ar flow rates 30, 200, and 200 sccm and the same growth duration 60 min, direct graphene growth is performed on a 600 nm SiO<sub>2</sub>/Si substrate. The growth conditions of the sample are described in Sec. II. The SEM image of the graphene grown on SiO<sub>2</sub> surface is shown in Fig. 6(a). Unlike the case on the sapphire substrates, the graphene that grows on the SiO<sub>2</sub>/Si substrate shows a very rough surface. The possible mechanism responsible for this phenomenon may lie on the different surface roughnesses of the substrates after the high-temperature

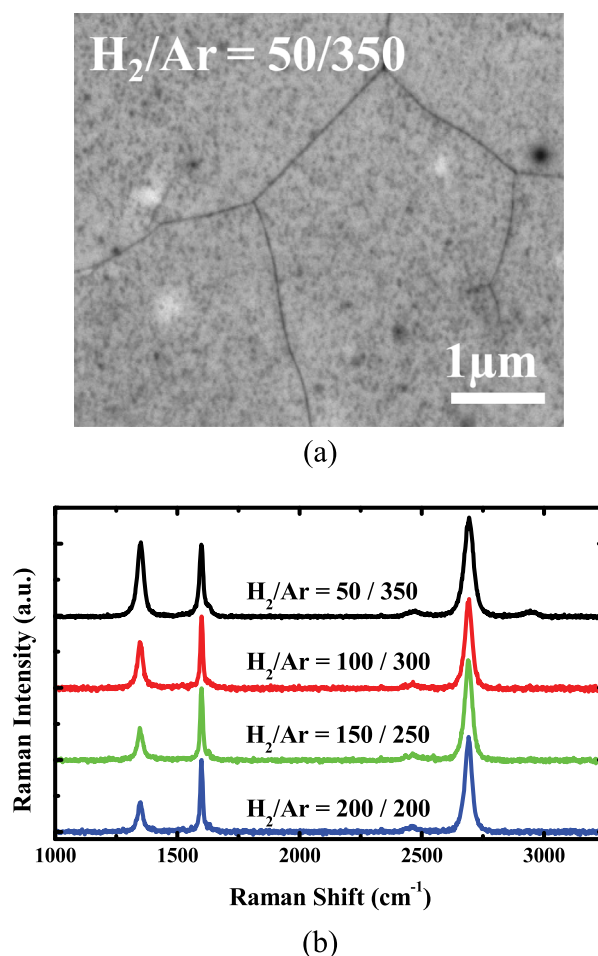


FIG. 5. (a) The SEM image of the sample prepared under H<sub>2</sub>/Ar flow ratio 50/350 and (b) the Raman spectra of the sample grown under different H<sub>2</sub>/Ar flow ratios.

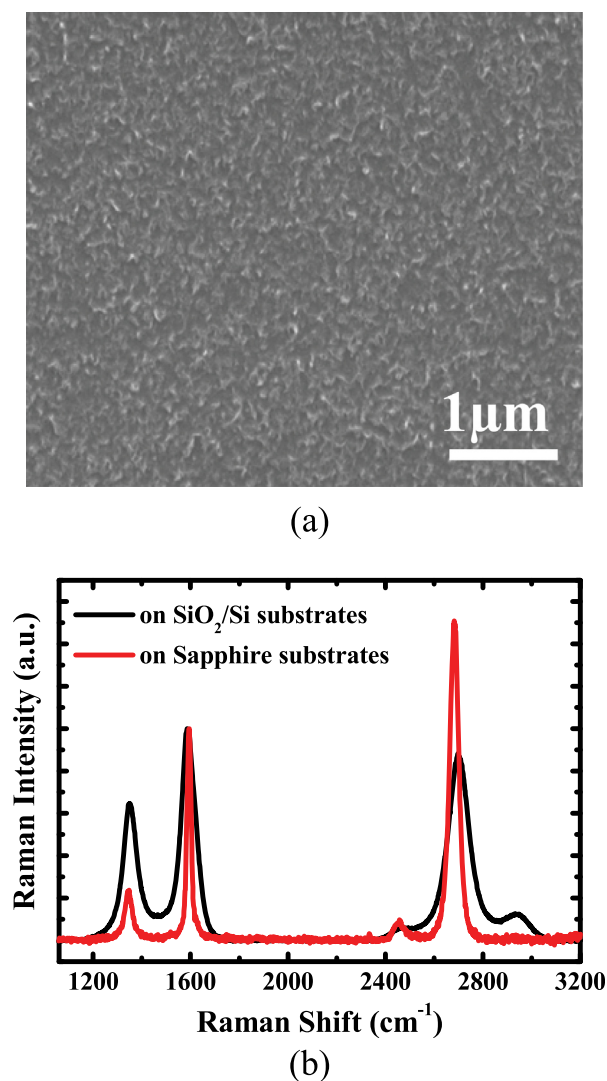


FIG. 6. (a) The Raman spectrum and (b) the SEM image of the direct graphene growth sample on a 600 nm  $\text{SiO}_2/\text{Si}$  substrate.

growth procedure. The surface roughnesses of  $\text{SiO}_2/\text{Si}$  and sapphire substrates are 0.13 and 0.05 nm, respectively, after 1100 °C annealing for 60 min under Ar environment. Therefore, the graphene flakes would not uniformly distribute over rougher surfaces. The same mechanism would also affect the crystalline quality of the graphene film. The Raman spectra of the two samples grown under the same growth conditions but on the two different substrates are shown in Fig. 6(b). As shown in the figure, significant difference can be observed on the FWHM of the 2D- and the D-peak intensities. The 2D-peak FWHM of the graphene film grown on sapphire substrates is  $43 \text{ cm}^{-1}$ , while for the film grown on the  $\text{SiO}_2/\text{Si}$  substrate, the 2D-peak FWHM value is increased to  $97 \text{ cm}^{-1}$ , which indicates the graphene grown on  $\text{SiO}_2$  surface has thicker layer number. Also observed in the figure is the much higher D-peak intensity of the graphene film grown on the  $\text{SiO}_2/\text{Si}$  substrate. The results suggest that although the directly grown graphene film is composed by graphene flakes, the limited lateral growth of

overlapped graphene flakes would still benefit larger graphene flake growth. Graphene deposition preference could be the other key issue for uniform graphene growth. In this case, the rougher surface and different substrate choices would result in a smaller graphene flakes and non-continuous films.

#### IV. CONCLUSIONS

In conclusion, the growth mechanism of the directly formed graphene on the dielectric substrate has been investigated. By changing the growth conditions, the formation mechanism of the graphene films directly on sapphire substrates is investigated. With the removal of the required film transferring procedure for conventional graphene films grown on Cu foil or metal etching process for underneath graphene films, the direct graphene growth method on dielectric substrates has provided a ready approach for practical applications.

#### ACKNOWLEDGMENTS

This work was supported in part by the National Science Council Projects NSC 102-2221-E-001-032-MY3 and NSC 102-2622-E-002-014 and Nano-project founded by Academia Sinica.

- <sup>1</sup>K. S. Novoselov, A. K. Geim, S. V. Morozov, D. Jiang, Y. Zhang, S. V. Dubonos, I. V. Grigorieva, and A. A. Firsov, *Science* **306**, 666 (2004).
- <sup>2</sup>Y. M. Lin, C. Dimitrakopoulos, K. A. Jenkins, D. B. Farmer, H.-Y. Chiu, A. Grill, and Ph. Avouris, *Science* **327**, 662 (2010).
- <sup>3</sup>X. Li, W. Cai, J. An, S. Kim, J. Nah, D. Yang, R. Piner, A. Velamakanni, I. Jung, E. Tutuc, S. K. Banerjee, L. Colombo, and R. S. Ruoff, *Science* **324**, 1312 (2009).
- <sup>4</sup>K. S. Kim, Y. Zhao, H. Jang, S. Y. Lee, J. M. Kim, K. S. Kim, J.-H. Ahn, P. Kim, J.-Y. Choi, and B. H. Hong, *Nature* **457**, 706 (2009).
- <sup>5</sup>X. Li, Y. Zhu, W. Cai, M. Borysiak, B. Han, D. Chen, R. D. Piner, L. Colombo, and R. S. Ruoff, *Nano Lett.* **9**, 4359 (2009).
- <sup>6</sup>C. Y. Su, A. Y. Lu, C. Y. Wu, Y. T. Li, K. K. Liu, W. Zhang, S. Y. Lin, Z. Y. Juang, Y. L. Zhong, F. R. Chen, and L. J. Li, *Nano Lett.* **11**, 3612 (2011).
- <sup>7</sup>S. J. Byun, H. Lim, G. Y. Shin, T.-H. Han, S. H. Oh, J. H. Ahn, H. C. Choi, and T. W. Lee, *J. Phys. Chem. Lett.* **2**, 493 (2011).
- <sup>8</sup>M. Y. Lin, Y. S. Sheng, S. H. Chen, C. Y. Su, L. J. Li, and S. Y. Lin, *J. Vac. Sci. Technol. B* **29**, 061202 (2011).
- <sup>9</sup>A. Ismach, C. Druzgalski, S. Penwell, A. Schwartzberg, M. Zheng, A. Javey, A. J. Bokor, and Y. Zhang, *Nano Lett.* **10**, 1542 (2010).
- <sup>10</sup>H. J. Song, M. Son, C. Park, H. Lim, M. P. Levendorf, A. W. Tsen, J. Park, and H. C. Choi, *Nanoscale* **4**, 3050 (2012).
- <sup>11</sup>G. Wang, M. Zhang, Y. Zhu, G. Ding, D. Jiang, Q. Guo, S. Liu, X. Xie, P. K. Chu, Z. Di, and X. Wang, *Sci. Rep.* **3**, 2465 (2013).
- <sup>12</sup>S. Lee, K. Lee, and Z. Zhong, *Nano Lett.* **10**, 4702 (2010).
- <sup>13</sup>M. A. Pimenta, G. Dresselhaus, M. S. Dresselhaus, L. G. Cançado, A. Jorio, and R. Saito, *Phys. Chem. Chem. Phys.* **9**, 1276 (2007).
- <sup>14</sup>A. Gupta, G. Chen, P. Joshi, S. Tadigadapa, and P. C. Eklund, *Nano Lett.* **6**, 2667 (2006).
- <sup>15</sup>L. Gan and Z. Luo, *ACS Nano* **7**, 9480 (2013).
- <sup>16</sup>Z. Li, P. Wu, C. Wang, X. Fan, W. Zhang, X. Zhai, C. Zeng, Z. Li, J. Yang, and J. Hou, *ACS Nano* **5**, 3385 (2011).
- <sup>17</sup>I. Vlasiouk, M. Regmi, P. Fulvio, S. Dai, P. Datskos, G. Eres, and S. Smirnov, *ACS Nano* **5**, 6069 (2011).
- <sup>18</sup>H. Bi, S. Sun, F. Huang, X. Xie, and M. Jiang, *J. Mater. Chem.* **22**, 411 (2012).